Chemical Engineering Journal 145 (2009) 371–376

Contents lists available at ScienceDirect

Chemical Engineering Journal

journal homepage: www.elsevier.com/locate/cej

Effect of initial solution apparent pH on nano-sized nickel catalysts in *p*-nitrophenol hydrogenation

Rizhi Chen [a], Qinqin Wang [a], Yan Du [b], Weihong Xing [a], Nanping Xu [a,*]

[a] *State Key Laboratory of Materials-Oriented Chemical Engineering, College of Chemistry and Chemical Engineering, Nanjing University of Technology, No. 5 Xinmofan Road, Nanjing 210009, China*
[b] *College of Environmental Sciences, Nanjing University of Technology, Nanjing 210009, China*

ARTICLE INFO

Article history:
Received 10 March 2008
Received in revised form 21 July 2008
Accepted 28 July 2008

Keywords:
Apparent pH effect
Nano-sized nickel
p-Nitrophenol
Catalytic hydrogenation

ABSTRACT

The effect of initial solution apparent pH (pH_a) on nano-sized nickel in the catalytic hydrogenation of *p*-nitrophenol to *p*-aminophenol was investigated in detail. Experimental results show that the catalytic activity of the nano-sized nickel shows a strong dependence on the initial solution pH_a, and is the highest at the initial solution pH_a 4.8. At lower or higher pH_a values the nano-sized nickel will obviously deactivate, but the deactivation mechanisms are fully different. With respect to the former, the nickel dissolution and the strong adsorption of the complex compound of nickel ion and *p*-nitrophenol on the surface of nano-sized nickel are the main reasons. The severe agglomeration of nickel particles also causes the deactivation of nickel used at the initial solution pH_a 1.6. For the latter the main reasons are the formation of nickel hydroxide surface species and the decrease of *p*-nitrophenol adsorption on the hydrogenation sites.

1. Introduction

p-Aminophenol is of great commercial importance as an intermediate for the preparation of analgesic and antipyretic drugs [1–4]. In view of the growing demands for *p*-aminophenol, direct catalytic hydrogenation of *p*-nitrophenol to *p*-aminophenol becomes important, because this could be an efficient and environmental friendly process [5].

Up to now, some works have been reported on the liquid phase *p*-nitrophenol hydrogenation over Raney nickel [6], nano-sized nickel [6] and several noble metal catalysts such as Pt/C [5]. The catalytic properties of nano-sized nickel have been proven to be superior to those of Raney nickel in this reaction in our previous works [6]. The effects of the reactant concentration, pressure and reaction temperature on the reaction rate have been also investigated [6]. However, more information on the influence of different parameters such as pH, mixing speed and catalyst concentration on the course of the hydrogenation reaction is still needed to understand the behavior of the nano-sized catalysts. It is well accepted that the initial solution pH can significantly affect the catalytic properties of metal catalysts [7,8], and the influence trend is variant for different catalytic reactions. Li et al. found in the catalytic wet air oxidation of 2-chlorophenol (2-CP) over Ru/ZrO_2 catalysts, the conversion of 2-CP and the TOC removal increased when increasing the initial pH from 2 to 10, and the initial 2-CP conversion rate went on increasing but the TOC abatement stayed almost constant as increasing the initial pH from 10 to 12 [7]. It was found by Feng et al. in the degradation of Orange II using two clay-based Fe nanocomposites as catalysts that the activity of the catalysts decreased as the initial solution pH increased [8]. Up to date, there are few reports on the investigation of the effect of the initial solution pH on nano-sized nickel catalysts in detail.

The present paper focuses on the initial solution pH_a effect on the catalytic hydrogenation of *p*-nitrophenol to *p*-aminophenol using nano-sized nickel as catalyst. After the reaction, the concentration of nickel element in the mother solution was measured by ICP. The used nickel catalysts were characterized by XRD, FTIR, FESEM, BET and XPS. At the same time, the reasons of the deactivation of nano-sized nickel at lower or higher initial solution pH_a were discussed.

2. Experimental

2.1. Catalyst preparation and characterization

The nano-sized nickel catalysts were prepared by the improved chemical reduction method in a continuous reactor according to Du et al. [6]. X-ray powder diffraction (XRD) patterns were obtained on a Bruker D8 instrument with Ni-filtered Cu Kα radiation ($\lambda = 0.154$ nm) at 40 kV and 30 mA, employing a scanning rate of $0.05^\circ\ s^{-1}$ in the 2θ range from 20° to 80°. The morphology and particle size of the samples were observed by field emission scan-

---

[*] Corresponding author. Tel.: +86 25 83587174; fax: +86 25 83300345.
E-mail address: npxu@njut.edu.cn (N. Xu).

1385-8947/$ – see front matter © 2008 Published by Elsevier B.V.
doi:10.1016/j.cej.2008.07.042

ning electron microscopy (FESEM, LEO1530VP). BET surface areas of the samples were measured by N_2 adsorption on a BELSORP-II adsorption apparatus. Before measurement, each sample was degassed at 100 °C for 3 h. The XPS characterization was conducted on a Thermo ESCALAB 250 system with a monochromatized Al Kα radiation ($h\nu = 1486.6$ eV) at 10 kV and 20 mA. The residual pressure in the analysis chamber was about 10^{-6} Pa. The analyzer was operated in the constant analyzer energy (CAE) mode with a pass energy of 20 eV at a 0.05 eV step. The C_{1s} signal (284.6 eV) was used to calibrate the binding energies. The surface concentrations of Ni and O were determined with the integrated peak areas of the Ni_{2p} and O_{1s} adjusted by their sensitivity factors. FTIR spectra were recorded with a Nicolet 380 spectrometer. All the spectra were carried out at room temperature after the samples were pressed to wafer with the help of KBr.

2.2. *Hydrogenation experiments*

The catalytic hydrogenation of *p*-nitrophenol to *p*-aminophenol was carried out in a 300 mL stainless steel autoclave equipped with a magnetically driven impeller. After 0.5 g catalysts and 14 g *p*-nitrophenol in 163 mL ethanol–water mixture consisted of 143 mL 95% ethanol and 20 mL deionized water were introduced into the autoclave, the mixture was stirred until the *p*-nitrophenol was dissolved, and then the initial pH_a of the mother solution was adjusted to a desired value in the range of 1.5–9.5 by adding the appropriate amount of HNO_3 or NaOH. The pH_a value of the mixture was measured with a PHS-3C pH meter (Shanghai Precision & Scientific Instrument Co., Ltd., Shanghai, China). Calibration employed standard buffer solutions (pH 4.0, 6.86 and 9.18) before each pH_a measurement. The preliminary experiments proved that the HNO_3 or NaOH did not interfere with the *p*-nitrophenol to form other materials in the studied pH_a range under the condition of no addition of nano-sized nickel into reaction solution. The reactor was sealed and purged with hydrogen five times to remove the air, and then heated to a desired temperature under low mixing. After the temperature reached the set value, hydrogen gas was introduced into the reactor to a set level, and the contents were mixed at 320 rpm. The preliminary experiments proved that the hydrogenation reaction at mixing speed above 300 rpm is not influenced by external diffusion. Last, the hydrogenation reaction was performed at 102 °C and 1.65 MPa. After 1-h reaction, the catalysts were separated from the reaction solution, thoroughly washed with ethanol and dried at room temperature for the followed characterizations. The concentration of nickel element in the mother solution was analyzed by inductively coupled plasma emission spectroscopy (ICP, Optima 2000DV). Specimens for ICP analysis were extracted with nitric acid for 10 min at a temperature of 200 °C and at a power of 800 W on a CEM MARS instrument. The products were analyzed by a HPLC system (Agilent 1100 Series, USA) equipped with a diode array detector (DAD) and an auto-sampler. Chromatographic separations were performed at 35 °C using a ZORBAX Eclipse XDB-C18, 5 μm, 4.6 mm × 250 mm column. A mobile phase composed of 80% methanol and 20% water at a flow rate of 1 ml min^{-1} was used. In this paper, the catalytic activity of the nano-sized nickel is expressed by reaction rate defined as the amount of hydrogen consumed per minute and per gram of catalyst [6].

3. Results and discussion

3.1. *Effect of the initial solution pH_a on the catalytic activity of nano-sized nickel*

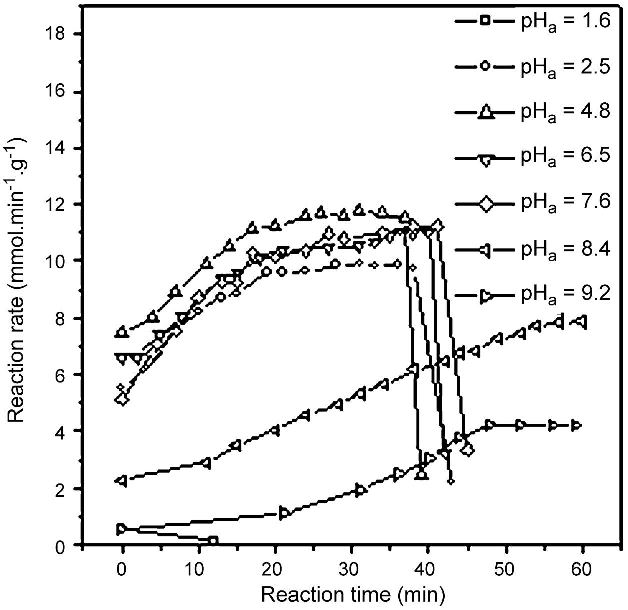

Fig. 1. Effect of the initial solution pH_a on the reaction rate of the catalytic hydrogenation of *p*-nitrophenol to *p*-aminophenol using nano-sized nickel as catalyst.

The effect of the initial solution pH_a on the hydrogenation of *p*-nitrophenol to *p*-aminophenol catalyzed by nano-sized nickel at a concentration of 3.07 g L^{-1} is presented in Fig. 1. Apparently, the initial solution pH_a can significantly influence the catalytic activity of the nano-sized nickel. The catalytic activity is the highest at the initial solution pH_a 4.8 (no addition of HNO_3 or NaOH), and decreases at lower or higher pH_a values. For examples, the catalytic activity (expressed as the reaction rate at about 20 min) at the initial solution pH_a 2.5 is 85.2% of that at the initial solution pH_a 4.8; by increasing the initial solution pH_a value from 4.8 to 9.2, the catalytic activity (expressed as the reaction rate at about 20 min) decreases from 11.28 to 1.10 mmol min^{-1} g^{-1}. It can also be seen, when HNO_3 is added into the reaction solution the catalytic activity decreases with a decrease of pH_a value, and the catalytic activity at the initial solution pH_a 1.6 is very low and decreases close to zero along with reaction proceeding, which indicates the nano-sized nickel has been completely deactivated. The catalytic activity almost keeps stable when the initial solution pH_a increases from 6.5 to 7.6 and then decreases obviously by further increasing the initial solution pH_a. These results show that the nano-sized nickel will obviously deactivate at lower or higher pH_a values and the feasible initial solution pH_a value for the hydrogenation of *p*-nitrophenol to *p*-aminophenol over nano-sized nickel catalysts is from 2.5 to 7.6.

It is noted from Fig. 1 that with respect to the *p*-nitrophenol hydrogenation at the initial solution pH_a 2.5, 4.8, 6.5, 7.6, respectively, the reaction rate first increases with time, then becomes stabilized, and then decreases. The first stage corresponds to the activation of nano-sized nickel. The second and third stages are related to the concentration of *p*-nitrophenol, namely that the reaction rate is not affected by *p*-nitrophenol concentration except at lower concentrations [5]. When the amount of NaOH added into the reaction solution increases, i.e. the initial solution pH_a value increases from 4.8 up to 9.2, the initial reaction rate of *p*-nitrophenol hydrogenation gradually decreases, possibly due to that the increased hydroxyl ion could affect the activation of nano-sized nickel. For instance, the initial reaction rate at the initial solution pH_a 9.2 is only 7.3% of that at the initial solution pH_a 4.8.

HPLC analysis results show that the initial solution pH_a does not influence significantly the selectively of the nano-sized nickel in the catalytic hydrogenation of *p*-nitrophenol to *p*-aminophenol.

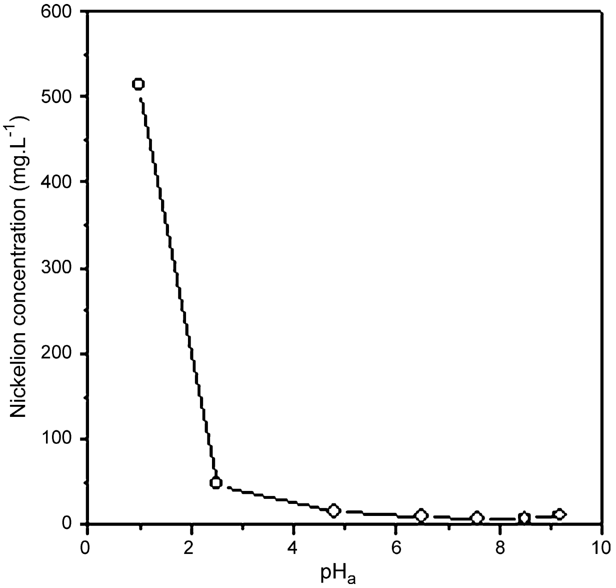

Fig. 2. Concentration of nickel ion in the mother solution at different initial solution pH$_a$.

3.2. Investigation of deactivation mechanisms

In order to investigate the deactivation mechanisms of nano-sized nickel, the used nickel catalysts were characterized by XRD, FTIR, FESEM, BET and XPS.

3.2.1. Deactivation at lower initial solution pH$_a$

Fig. 2 plots the concentration of nickel ion in the mother solution as a function of the initial solution pH$_a$ value. Dissolution of nickel is significant for pH$_a$ 1.6 and decreases obviously with an increase of pH$_a$ value. As presented in Fig. 3, the reaction rate of *p*-nitrophenol hydrogenation almost decreases linearly with a decrease of nickel catalyst concentration in the studied experimental range. Therefore, nickel dissolution should be one of the main reasons for the decrease of catalytic activity of nickel used at lower pH$_a$. In the study of Biella et al. [9], metal leaching was proved to be more consistent as pH decreased and corresponded to a gradual decrease in activity. Besson and Gallezot [10] thought that catalyst leaching in the reaction medium was the main cause of deactivation in liquid phase reactions.

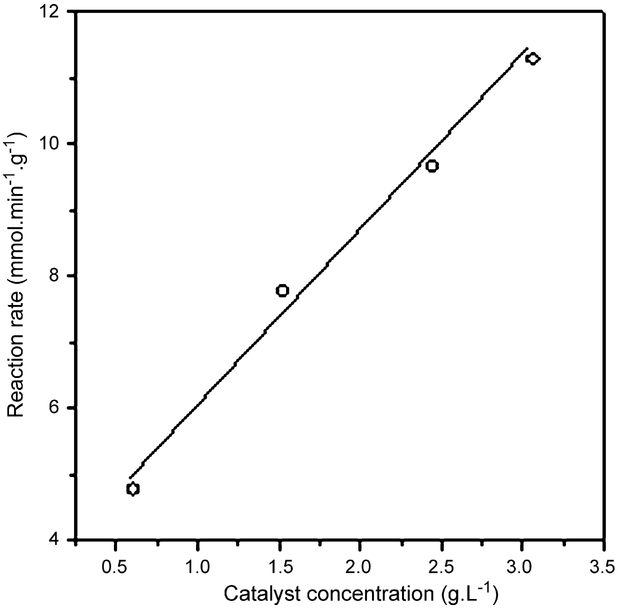

Fig. 3. Effect of catalyst concentration on the reaction rate (at about 20 min) of the catalytic hydrogenation of *p*-nitrophenol to *p*-aminophenol at the initial solution pH$_a$ 4.8.

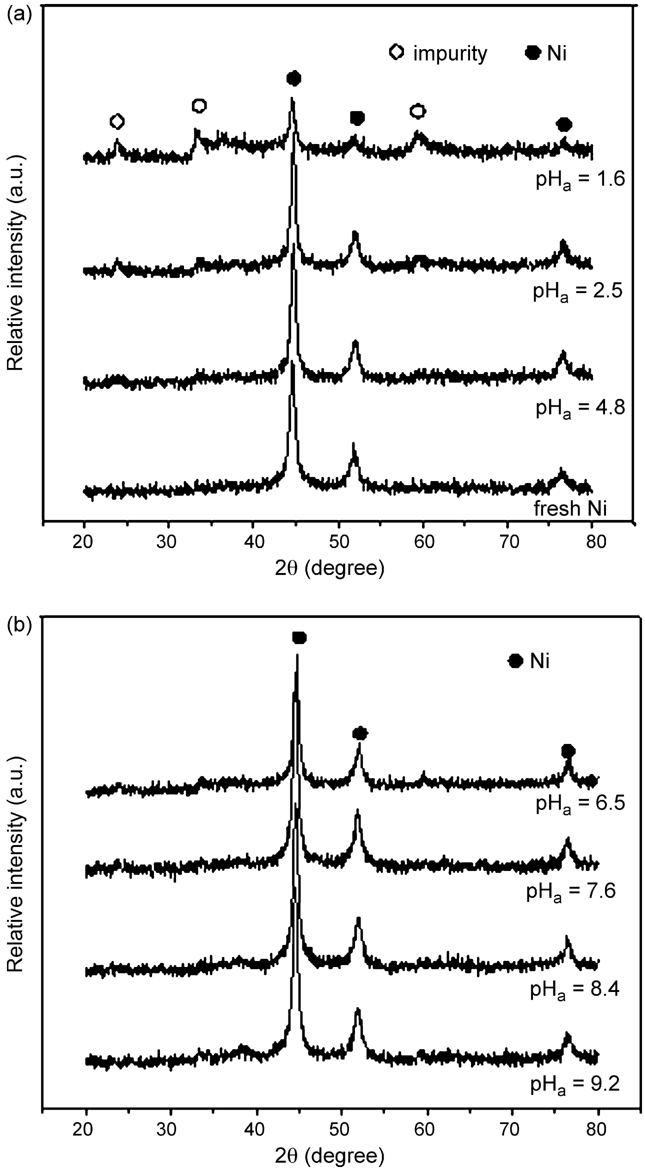

Fig. 4. XRD patterns of the samples: (a) fresh Ni and Ni used at pH$_a$ from 1.6 to 4.8; (b) Ni used at pH$_a$ from 6.5 to 9.2.

The XRD patterns of nickel used at the initial solution pH$_a$ 1.6, 2.5 and 4.8 are presented in Fig. 4(a), and the result of fresh nickel is also presented for comparison. For the nickel used at the initial solution pH$_a$ 4.8, the composition is almost elementary nickel ($2\theta = 44.5°$, 52.0° and 76.9°, corresponding to the Miller index (1 1 1), (2 0 0), (2 2 0), respectively). When the initial solution pH$_a$ decreases to 2.5, the main composition of used nickel is still elementary nickel and at the same time some impurity peaks ($2\theta = 23.8°$, 33.2° and 59.3°) have been observed. With a further decrease of pH$_a$, the impurity peaks become obvious. The impurity adsorbed strongly on the surface of nano-sized nickel should be one of the main reasons for the deactivation of nickel used at lower pH$_a$. In order to probe into the composition of the impurity, the nickel sample used at the initial

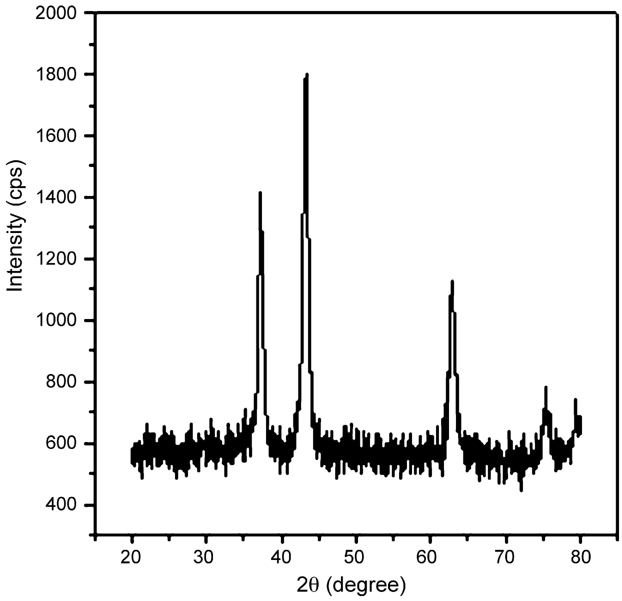

Fig. 5. XRD pattern of Ni used at pH_a 1.6 after calcined at 500 °C for 4 h.

solution pH_a 1.6 was calcined in stagnant air at 500 °C for 4 h, and then characterized by XRD. As shown in Fig. 5, five characteristic peaks are observed in the 2θ ranges from 20° to 80°, which are all consisted of those of NiO phase, proving the sole existence of NiO particles. The result shows the impurity can be burned away at 500 °C, revealing it should be some organic compounds. To further investigate the impurity composition the nickel sample used at the initial solution pH_a 1.6 was characterized by FTIR, and the result is shown in Fig. 6. The FTIR spectrum of fresh nickel is also shown in Fig. 6. Compared to the fresh nickel, some new adsorption bands are observed. The band observed at 470 cm^{-1} can be assigned to the out-of-plane CO vibration coupled with the phenyl ring torsion [11]. The band at 648 cm^{-1} might be assignable to the in-plane ring deformation coupled with NO_2 scissoring vibration [11]. These 1117, 1167, 1296 and 1488 cm^{-1} bands are ascribed to the CH in-plane bending vibrations. The band at 1346 cm^{-1} corresponds to the symmetric NO_2 stretching vibration. The 1384 and 1587 cm^{-1} bands can be attributed to the C=C aromatic stretching vibrations. The FTIR results indicate the impurity contains CO group, NO_2 group and phenyl ring. On the other hand, no impurities form at higher pH_a values, as shown in Fig. 4(b). So we think the impurity might be the complex compound of *p*-nitrophenol and nickel ion, and form in the following way: at lower pH_a values some nickel particles are dissolved to form nickel ion (as shown in Fig. 2) and subsequently the nickel ion interact with the *p*-nitrophenol to form a complex compound. In addition, the recovered nickel particles after washing and drying used at the initial solution pH_a 1.6 were black yellow in color, and the impurity adsorbed on the nickel surface could not be eliminated by thoroughly washing with ethanol, however, the *p*-nitrophenol adsorbed on the nickel surface could be eliminated by thoroughly washing with ethanol, indicating that the impurity adsorbed on the nickel surface was not the *p*-nitrophenol; while the recovered nickel particles after washing and drying used at the initial solution pH_a 4.8 were black in color like that of the fresh catalyst particles. The phenomena were in agreement with the results of FTIR and XRD.

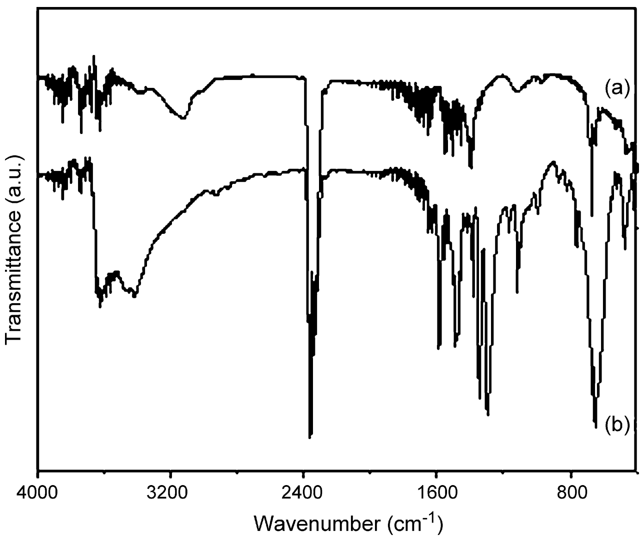

Fig. 6. FTIR spectra of the samples: (a) fresh Ni; (b) Ni used at pH_a 1.6.

The FESEM micrographs with different amplified factor of the nickel used at the initial solution pH_a 1.6 are shown in Fig. 7(a). It is noted from the FESEM micrograph with an amplified factor of 80,000 compared to the nickel used at the initial solution pH_a 4.8 as shown in Fig. 7(b), the particle size of nickel is obviously smaller. Biella et al. [9] also found that when metal leaching increased the particle size decreased. As observed from the FESEM micrograph with an amplified factor of about 2500, in comparison with the nickel used at the initial solution pH_a 4.8, the agglomeration of nickel particles is obvious, possibly because of the smaller particle size [12] and adsorbed impurity. This is also verified by BET analysis, as shown in Table 1. The specific surface area of the nickel used at the initial solution pH_a 1.6 is 6.8 $m^2\,g^{-1}$, only about 31% that of the nickel used at the initial solution pH_a 4.8. The agglomeration of nickel particles is responsible for lowering the catalytic activity for the hydrogenation reaction at the initial solution pH_a 1.6. No obvious difference occurs in the specific surface area of the nickel used at the initial solution pH_a 2.5 and 4.8.

The XPS characterization results of the nickel used at the initial solution pH_a 1.6 are shown in Table 1 and Fig. 8(a). In comparison with the nickel used at the initial solution pH_a 4.8, the Ni_{2p} spectrum peaks intensity and the surface O/Ni atomic ratio of the nickel used at the initial solution pH_a 1.6 are lower, possibly because with respect to the former no impurity adsorbed on the nickel surface during the reaction, and the O species was mainly from the nickel oxide formed during the after-treatment, while with respect to the latter the complex compound of nickel ion and *p*-nitrophenol would form during the reaction and adsorb on the nickel surface, and the O species was mainly from the complex compound.

According to above analysis, it may be concluded that the deactivation of nano-sized nickel used at lower pH_a is a combination effect of the nickel dissolution and the strong adsorption of impurity on the surface of nano-sized nickel; the severe agglomeration of nickel particles also causes the deactivation of nickel used at the initial solution pH_a 1.6.

3.2.2. Deactivation at higher initial solution pH_a

The XRD patterns of nickel used at the initial solution pH_a 6.5, 7.6, 8.4 and 9.2 presented in Fig. 4(b) show that these used nickel catalysts are chiefly composed of elementary nickel and no impurities exist on their surface due to no nickel ion in the mother solutions (as shown in Fig. 2).

It is found by comparing the FESEM micrographs of nickel used at the initial solution pH_a 4.8 and 9.2 shown in Fig. 7(b) and (c), no obvious difference exists. Table 1 shows that the specific surface area of the nickel used at the initial solution pH_a 9.2 is almost the same as that of the nickel used at the initial solution pH_a 4.8.

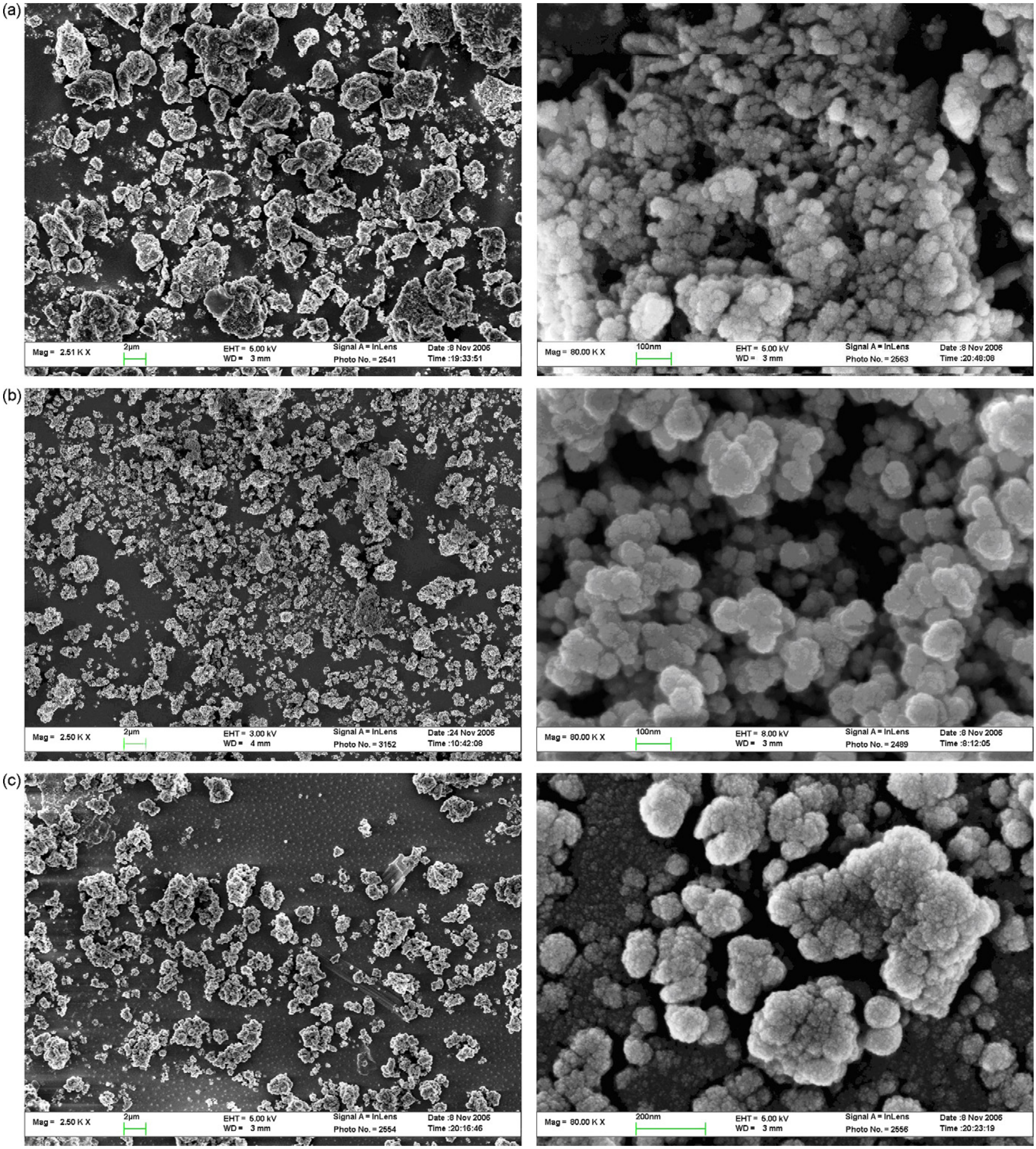

Fig. 7. FESEM of the samples: (a) Ni used at pH_a 1.6; (b) Ni used at pH_a 4.8; (c) Ni used at pH_a 9.2.

These results indicate the agglomeration of nickel particles changed slightly when NaOH was added into the reaction solution and would not cause the deactivation of nano-sized nickel.

Fig. 8(c) and Table 1 show the XPS characterization results of the nickel used at the initial solution pH_a 9.2. Compared to the nickel used at the initial solution pH_a 4.8, the Ni_{2p} spectrum of the nickel used at the initial solution pH_a 9.2 has basic similar profile, as shown in Fig. 8(b) and (c), however the peaks intensity is obviously lower, indicating the lower nickel amount on the surface of the used nickel. This would make the catalytic activity decrease to some extent. The surface O/Ni atomic ratio of the nickel used at the initial solution pH_a 9.2 is higher than that of the nickel used at the initial solution pH_a 4.8 possibly due to that the nickel hydroxide surface species would form on the nickel surface when NaOH was added into the reaction solution and the O species was mainly from the nickel hydroxide [13]. According to the study of Hernández et al. [13], the isoelectric point (IEP) of nickel was at 3.5–4, and above the IEP the nickel hydroxide surface species would form. Therefore,

Table 1
Characterization results of used nickel samples

Samples	Ni used at pH_a 1.6	Ni used at pH_a 4.8	Ni used at pH_a 9.2
Binding energy of $Ni_{2p3/2}$ (eV)	855.50	855.35	855.35
Surface O/Ni atomic ratio	1.67	1.98	2.18
Specific surface area ($m^2\ g^{-1}$)	6.8	22.0	24.1

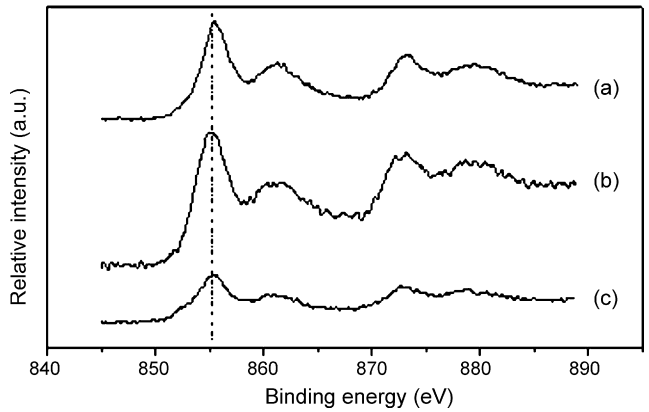

Fig. 8. XPS spectra of Ni_{2p} for different samples: (a) Ni used at pH_a 1.6; (b) Ni used at pH_a 4.8; (c) Ni used at pH_a 9.2.

in this work, when the initial solution pH_a was higher, the nickel hydroxide species would form on the nickel surface. At the same time, under the studied reaction conditions, the reduction of nickel hydroxide to metallic nickel might be difficult, and as a result the nickel hydroxide species would occur on the nickel surface.

Solution pH influences the ionization state of the Ni surface. At pH values lower than about 3.5, which are the point of zero charge for Ni [13], the Ni surface becomes positively charged, while at pH values greater than about 3.5 it becomes negatively charged. *p*-Nitrophenol is a weak acid and has a dissociation constant (pK_a) value of 7.15 [14]. Thus, in alkaline conditions *p*-nitrophenol is predominantly present in the dissociated form, and increase in pH causes increase in the dissociation of *p*-nitrophenol. Therefore, alkaline conditions would make the electrostatic repulsion between the negatively charged Ni surface and the anions, resulting in decreased adsorption of *p*-nitrophenol on the hydrogenation sites and consequently in decreased catalytic activity. Bangun and Adesina [15] found that the degradation rate of sodium oxalate using commercial titania as the catalyst dropped almost exponentially with increase in slurry pH. They also thought this was attributed to the increased density of negatively charged sites at high pH values.

Through above analysis we think that the deactivation of nano-sized nickel used at higher pH_a is mainly caused by the formation of nickel hydroxide surface species and the decrease of *p*-nitrophenol adsorption on the hydrogenation sites.

4. Conclusions

In this work, the effect of initial solution pH_a on nano-sized nickel in *p*-nitrophenol hydrogenation was studied in a laboratory-scale batch-slurry reactor. It has been demonstrated that the initial solution pH_a can significantly influence the catalytic activity of the nano-sized nickel, and almost has no influence on its selectivity. The nano-sized nickel shows the highest catalytic activity at the initial solution pH_a 4.8 (no addition of HNO_3 or NaOH). When HNO_3 is added into the reaction solution the catalytic activity decreases with a decrease of pH_a value, and the nano-sized nickel has been completely deactivated at the initial solution pH_a 1.6. The deactivation of nano-sized nickel used at lower pH_a is a combination effect of the nickel dissolution and the strong adsorption of the complex compound of nickel ion and *p*-nitrophenol on the surface of nano-sized nickel; the severe agglomeration of nickel particles also causes the deactivation of nickel used at the initial solution pH_a 1.6. When NaOH is added into the reaction solution, the catalytic activity almost keeps stable at the initial solution pH_a varying from 6.5 to 7.6 and then decreases obviously by further increasing the initial solution pH_a. The formation of nickel hydroxide surface species and the decrease of *p*-nitrophenol adsorption on the hydrogenation sites are the main reasons of the deactivation of nano-sized nickel used at higher pH_a. Our study clarifies that the feasible initial solution pH_a value for the hydrogenation of *p*-nitrophenol to *p*-aminophenol using nano-sized nickel as catalyst is from 2.5 to 7.6.

Acknowledgments

We acknowledge the supports of the National Basic Research Program (2003CB615702), the National High Technology Research and Development Program (2007AA06A402), the National Natural Science Foundation (20636020) and the Natural Science Foundation of Jiangsu Province (BK2006722) of China.

References

[1] Y. Du, H.L. Chen, R.Z. Chen, N.P. Xu, Poisoning effect of some nitrogen compounds on nano-sized nickel catalysts in *p*-nitrophenol hydrogenation, Chem. Eng. J. 125 (2006) 9.
[2] C.V. Rode, M.J. Vaidya, R. Jaganathan, R.V. Chaudhari, Hydrogenation of nitrobenzene to *p*-aminophenol in a four-phase reactor: reaction kinetics and mass transfer effects, Chem. Eng. Sci. 56 (2001) 1299.
[3] C.V. Rode, M.J. Vaidya, R.V. Chaudhari, Synthesis of *p*-aminophenol by catalytic hydrogenation of nitrobenzene, Org. Process Res. Dev. 3 (1999) 465.
[4] R.Z. Chen, Y. Du, W.H. Xing, N.P. Xu, The effect of titania structure on Ni/TiO_2 catalysts for *p*-nitrophenol hydrogenation, Chi. J. Chem. Eng. 14 (2006) 665.
[5] M.J. Vaidya, S.M. Kulkarni, R.V. Chaudhari, Synthesis of *p*-aminophenol by catalytic hydrogenation of *p*-nitrophenol, Org. Process Res. Dev. 7 (2003) 202.
[6] Y. Du, H.L. Chen, R.Z. Chen, N.P. Xu, Synthesis of *p*-aminophenol from *p*-nitrophenol over nano-sized nickel catalysts, Appl. Catal. A: Gen. 277 (2004) 259.
[7] N. Li, C. Descorme, M. Besson, Catalytic wet air oxidation of aqueous solution of 2-chlorophenol over Ru/zirconia catalysts, Appl. Catal. B: Environ. 71 (2007) 262.
[8] J. Feng, X. Hu, P.L. Yue, Effect of initial solution pH on the degradation of Orange II using clay-based Fe nanocomposites as heterogeneous photo-Fenton catalyst, Water Res. 40 (2006) 641.
[9] S. Biella, L. Prati, M. Rossi, Selective oxidation of D-glucose on gold catalyst, J. Catal. 206 (2002) 242.
[10] M. Besson, P. Gallezot, Deactivation of metal catalysts in liquid phase organic reactions, Catal. Today 81 (2003) 547.
[11] A.J. Abkowicz-Bieńko, Z. Latajka, D.C. Bieńko, D. Michalska, Theoretical infrared spectrum and revised assignment for *para*-nitrophenol. Density functional theory studies, Chem. Phys. 250 (1999) 123.
[12] B. Sun, P.G. Smirniotis, Interaction of anatase and rutile TiO_2 particles in aqueous photooxidation, Catal. Today 88 (2003) 49.
[13] N. Hernández, R. Moreno, A.J. Sánchez-Herencia, J.L.G. Fierro, Surface behavior of nickel powders in aqueous suspensions, J. Phys. Chem. B 109 (2005) 4470.
[14] H. Sayılkan, S. Erdemoĝlu, S. Sener, F. Sayılkan, M. Akarsu, M. Erdemoĝlu, Surface modification of pyrophyllite with amino silane coupling agent for the removal of 4-nitrophenol from aqueous solutions, J. Colloid Interf. Sci. 275 (2004) 530.
[15] J. Bangun, A.A. Adesina, The photodegradation kinetics of aqueous sodium oxalate solution using TiO_2 catalyst, Appl. Catal. A: Gen. 175 (1998) 221.